Mechanisms for agglomeration and deagglomeration following oblique collisions of wet particles

Carly M. Donahue, Robert H. Davis, Advait A. Kantak, and Christine M. Hrenya

Phys. Rev. E **86**, 021303 — Published 20 August 2012

DOI: 10.1103/PhysRevE.86.021303

Mechanisms for agglomeration and de-agglomeration following oblique collisions of wet particles

Christine M. Donahue, Robert H. Davis, Advait A. Kantak, and Christine M. Hrenya*
Department of Chemical and Biological Engineering, University of Colorado, Boulder, Colorado 80309-0424, USA
**corresponding author: hrenya@colorado.edu*

Previous studies on wetted, particle-particle collisions have been limited to head-on collisions, but in many-particle flows, collisions are inherently oblique. In this work, we explore such oblique collisions experimentally and theoretically. Whereas in normal collisions particles rebound only due to solid deformation, we observe in oblique collisions a new outcome where the particles initially form a rotating doublet, and then de-agglomerate at a later time due to "so-called" centrifugal forces. Surprisingly, we discover the essential role of capillary forces in oblique collisions even when the capillary number (viscous over capillary forces) is high. This recognition leads to the introduction of a dimensionless number, the centrifugal number (centrifugal over capillary forces), which together with the previously established Stokes number characterizes the regime map of outcomes. Unexpectedly, we observe a normal restitution coefficient greater than unity at large impact angles, the mechanism for which may also be observed in other agglomerating systems.

Individual particulates in a granular material are frequently assumed to be smooth, hard spheres [1]. However, real systems are often more complex. Sand on the beach, an oft-cited example of a granular material, often contains water that forms a cohesive bond between grains. Our focus here is on collisions between liquid-coated, solid particles. A plethora of such systems that exhibit agglomeration/de-agglomeration behavior exists in nature (e.g. pollen capture, avalanches, pollution) and industry (e.g. granulation, filtration, inhalers). Previous experiments on wetted collisions have involved normal (head-on) and oblique collisions between a particle and a wall [2-4], and normal collisions between two or three particles [5]. Here, we extend experiment and theory to particle-particle, oblique collisions. No understanding of agglomeration is complete without studying the rotational motion of two mobile particles, be it colloids or electrostatically charged particles. Furthermore, this doublet rotation gives rise to a host of new phenomena for wetted collisions, including an additional outcome (Fig. 1b) in which de-agglomeration stems solely from so-called centrifugal forces, and the observation of a normal restitution coefficient greater than unity (indicating that the normal, post-collisional, relative velocity is greater than its pre-collisional counterpart). The latter counter-intuitive behavior is not limited to wetted collisions, since it results from hysteresis in the initial and final separation distances, which may be exhibited in other agglomerating systems.

This work is targeted at low Reynolds number, Re (ratio of inertia to viscous forces in the liquid gap between particles) such that Stokes flow prevails. Previous low-Re work on wetted collisions indicated that the primary dimensionless parameter that dictates agglomeration vs. de-agglomeration is the Stokes number, $St_n = mv_{n,0}/6\pi\mu a^2$ (ratio of particle inertia to viscous force), where m is reduced mass of particles, $v_{n,0}$ is normal component of relative impact velocity, μ is liquid viscosity, and a is reduced radius. Experiments have shown

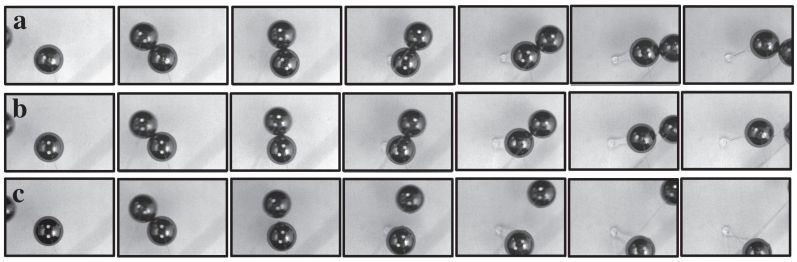

FIG. 1. Top-view of collisions that (a) stick (S), (b) stick-rotate-separate (SRS), and (c) bounce (B) for chrome steel spheres of 25.4 mm diameter, oil layer of 420 μm thickness and 12 Pa·s viscosity, and 45° impact angle. The only parameter changed between subfigures is impact velocity, such that the St_n is (a) 1.0, (b) 1.3, and (c) 1.5. The time between frames is (a) 79 ms, (b) 61 ms, and (c) 49 ms.

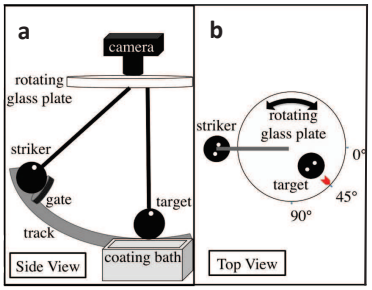

FIG 2. Schematic of pendulum setup: (a) side view and (b) top (camera) view.

that, if St_n is below a critical value, St_n^*, the two bodies stick (agglomerate), whereas, if $St_n > St_n^*$, they bounce (de-agglomerate), regardless of whether it is a normal particle-particle or oblique particle-wall collision [6]. The value of St_n^* is found theoretically via a coupling of hydrodynamics and solid mechanics [7] or measured directly in experiments [3].

Pendulums have proven useful for experiments of normal and oblique collisions, as they allow for small impact velocities [5,8,9] (as needed for Stokes flow with large particles). In this work, the striker and target particles are held by pendulum strings spaced one diameter apart (Fig. 2a). A coating bath is used to coat the target particle; the thickness of the coating at a given drainage time is measured using a high-resolution camera. The release position of the striker along the pendulum arc controls the impact velocity, and the string holding the target particle is attached to a rotating plate that controls the impact angle, θ_0 (Fig. 2b: $\theta_0 = 0°$: normal collisions; $\theta_0 = 90°$: perfectly tangential collisions). The pre- and post-collisional velocities are measured using high-speed imaging. Data collection ceases if the doublet is still agglomerated past 180°, since the pendulum strings cross, or if the angular velocity of the doublet reverses direction. As illustrated in Fig. 1, three possible outcomes are observed. At small St_n, the particles stick (S, Fig. 2a) due to viscous losses. At large St_n, the particles bounce (B, Fig. 1c) due to elastic deformation. These are the only two outcomes predicted and observed previously for normal collisions of two wet particles. However, at intermediate St_n for oblique collisions, the particles initially stick due to viscous losses, rotate through a substantial angle, and then separate due to centrifugal forces (SRS, Fig. 1b). Note that the "bounce" de-agglomeration mechanism is nearly instantaneous, whereas the "stick-rotate-separate" mechanism is relatively slow.

For further physical insight into this new de-agglomeration mechanism, we extended previous wetted-particle theories to our system [3,5,8]. Since Re is small ($Re = \rho v_{n,0} x_0/\mu < 0.04$ in experiments, where x_0 is liquid-layer thickness), viscous (dynamic) forces in the liquid bridge can be described by Stokes flow. Additionally, since the capillary number (ratio of viscous to capillary forces, $Ca = 3\mu a v_{n,0}/\sigma x_0 > 1500$, where σ is surface tension) is large, capillary (static) forces are relatively small. Previous experiments with pendulums, including oblique collisions of dry particles and wet particle-wall collisions, have shown that the strings exert negligible tension (in the plane of motion) on the particles [5,8,9]. However, we found

the inclusion of string tension critical to predicting the correct outcomes and trends, since the particles rotate through a significant angle before de-agglomerating, allowing for large string tension forces to act over a long period of time. Finally, based on recent experimental evidence [10], we do not presume cavitation occurs upon rebound and instead include the effect of fluid resistance.

Our theoretical description is based on Newton's equations of motion, including the centrifugal "force." Explicit forms for these governing equations are given in Table 1. In particular, momentum balances for both the translational and rotational motion are solved. The relevant forces in the former include the normal components of the lubrication force $F_{L,n}$ adapted for liquid-coated spheres [11] and the string tension $F_{S,n}$ derived such that its vertical component balances the weight [12], as well as the capillary force F_c between two wetted spheres [13] (only included in some model predictions, as discussed below). The relevant forces in the latter include the tangential components of the lubrication ($F_{L,t}$) [14] adapted for liquid-coated spheres [12] and the string-tension force ($F_{S,t}$). These equations are solved with an initial separation equal to the liquid-layer thickness x_0, an initial normal relative velocity $v_{n,0}$, and initial rotational velocities of $\omega_0 = v_{n,0} \tan\theta_0/(4a)$ and $\xi_0 = 0$ [12]. As the two particles approach each other, the pressure in the gap rapidly increases (squeezing), causing the particles to deform, which can lead to velocity reversal. If one of three reversal criteria [5] is met, namely (i) the glass-transition pressure, p_{gt}, is exceeded, (ii) the separation distance of the particle surfaces, x, equals the elasticity length scale [3], or (iii) x equals the surface roughness, then the particles reverse direction. Specifically, the relative velocity is reversed and multiplied by the dry restitution coefficient, e_{dry}, to account for the energy dissipated by the particles upon deformation. These criteria are identical to those of normal collisions, and are independent of potential reversal caused by centrifugal forces (which are not present in normal collisions). The particles then separate (de-agglomerate) from each other when x reaches x_0. Due to the lack of well-established data, p_{gt} is estimated based on the measured St_n^* [5]. More details on the theory can be found in [12], which is identical to the theory herein except that the role of the capillary force F_c is also considered in some cases here, as described below.

A regime map of outcomes is shown in Fig. 3. The theory and experiments show all three outcomes and are in good agreement except that the experimental S-SRS boundary occurs at higher θ_0 for a given St_n. Furthermore, the theory captures the experimental trends of how outcome boundaries change with physical parameters (e_{dry}, x_0, a, μ), the details of which are not included here for brevity. In Fig. 3, the value of St_n at which normal collisions ($\theta = 0°$) transition from stick to bounce (St_n^*) is equal to 1.4. For oblique collisions, the value of St_n^* also demarcates the transition between agglomeration and de-agglomeration for small impact angles ($\theta_0 \sim< 50°$). At large impact angles ($\theta_0 \sim> 50°$), however, St_n^* serves as the boundary between stick-rotate-separate and bounce. This inability of St_n^* to be used as a predictor of agglomeration vs. de-agglomeration for more oblique collisions is due to centrifugal forces, which are responsible for the ultimate de-agglomeration of the new stick-rotate-separate outcome.

In practical applications, pendulum strings are not present. To more realistically model these systems, we now consider a theory without string tension but with capillary forces. If two particles in a rotating doublet are to stick together, their relative velocity (and, lubrication suction force) eventually become zero. Since the centrifugal force continues to pull

Table 1: Theory Description

Kinematic Equations

$$m\frac{dv_n}{dt} = F_{L,n} + F_{S,n} + F_c - 4ma\omega^2 \qquad \frac{dx}{dt} = -v_n$$

$$4ma\frac{d\omega}{dt} = F_{L,t} + f_{S,t} + 2mv_n\omega \qquad \frac{d\beta}{dt} = \omega; \qquad \frac{8}{5}ma\frac{d\xi}{dt} = -F_{L,t}$$

Relevant Forces

Lubrication

$$F_{L,n} = -\frac{6\pi\mu a^2 v_n}{x}\left(1-\frac{x}{x_0}\right)^2$$

$$F_{L,t} = -8\pi\mu a^2(\omega-\xi)\ln\frac{2a}{x_0}$$

String Tension

$$F_{S,n} = \frac{8mga}{l}\sin^2\left(\frac{\beta}{2}\right)\sqrt{1-\frac{16a^2}{l^2}\sin^2\left(\frac{\beta}{2}\right)}$$

$$F_{S,t} = -\frac{4mga}{l}\sin(\beta)\sqrt{1-\frac{16a^2}{l^2}\sin^2\left(\frac{\beta}{2}\right)}$$

Capillary

$$F_c = 4\pi\sigma\exp\left(\frac{Ax}{2a}+B\right)+C$$

$$A = 1.1V^{-0.53}$$

$$B = (-0.34\ln V - 0.96)\phi^2 - 0.019\ln V + 0.48$$

$$C = 0.0042\ln V + 0.078$$

Here, n and t denote normal and tangential directions, respectively, $v_n(t)$ is relative normal velocity of two spheres, $x(t)$ is distance between their surfaces, $\omega(t)$ is angular velocity of doublet about its center of mass, $\xi(t)$ is angular velocity of each particle about its center, $\beta(t)$ is angle through which the doublet has rotated from initial contact, l is length of pendulum string, g is gravitational acceleration, V is liquid bridge volume non-dimensionalized by the particle radius cubed (assumed constant), and ϕ is contact angle of liquid with solid sphere (assumed zero). The lubrication force in the normal direction is the classic formula, corrected for finite film thickness [8]; the tangential component is approximated using the asymptotic analysis for nearly-touching, fully-immersed spheres [9], but modified by removing the constant term so that no hydrodynamic force exists on the doublet when in rigid-body motion ($\omega = \xi$). When the first kinematic equation is non-dimensionalized by $a\sigma$, the centrifugal number falls out from centrifugal force.

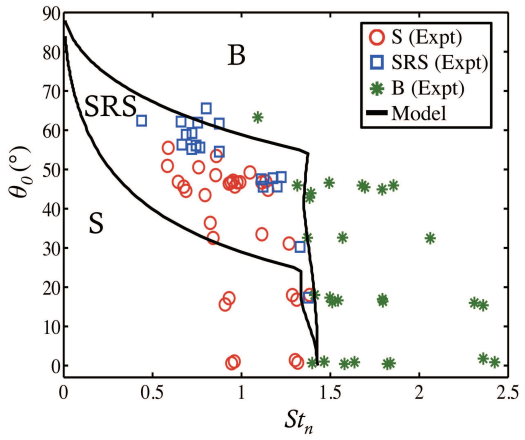

FIG. 3. Regime map of collisional outcomes for pendulum apparatus. Symbols represent experimental data and lines represent theory-based boundaries between outcomes for $e_{dry} = 0.99$, $x_0 = 420\mu m$, $x_b = 1\mu m$, $a = 0.63$ cm, $\mu = 12$ Pa·s, $m = 34$ g, $p_{gt} = 12$ MPa. Pendulum strings are responsible for sticking collisions at oblique angles ($\theta_0 > 0$).

such particles apart, another force must balance it for the particles to remain agglomerated. In untethered collision, the additional force is provided by capillary forces. Recall that, here, Ca is large, implying that capillary forces should be negligible [15]. Therefore, somewhat surprisingly, even when Ca is large, capillary forces are non-negligible for *oblique* collisions and thus included in the theory (but not in the theory for the experiments, since string tension overshadows capillary forces). The key roles of centrifugal and capillary forces in agglomeration and de-agglomeration processes were also considered by Petela [16], but for the very different case where the centrifugal force is due to rotation of the agglomerate caused by velocity gradients in the stirred, surrounding liquid.

In Fig. 4, we provide a regime map of outcomes by solving Newton's equations for the oblique collision of two particles without pendulum strings but with the capillary force included, for input parameters representative of granulation and other industrial applications.

De-agglomeration occurs when the liquid bridge ruptures at $x_f = 2aV^{1/3}$ [17]. It is important to note that while the shape of the boundary between stick and stick-rotate-separate is similar in Fig. 3 and 4a, the mechanisms for sticking (agglomeration) are surprisingly different. In both cases, if $St_n < St_n^*$, the particles initially agglomerate due to viscous forces and rotate as a doublet. The corresponding centrifugal force tends to pull the doublet apart. In Fig. 3, with pendulum strings, the centrifugal force is opposed by a lubrication suction force and string tension. In Fig. 4a, without pendulum strings, the centrifugal force is opposed by lubrication suction and the capillary force; without the capillary force, de-agglomeration would always occur for reasons described above. On the contrary, unlike oblique collisions, normal collisions are practically unaffected by the presence of capillary forces. Normal collisions still agglomerate for $St_n < St_n^*$, even when capillary forces are removed (as indicated by arrow pointing to $\theta_0 = 0$ in inset of Fig. 4a), consistent with previous theories [3,5,8].

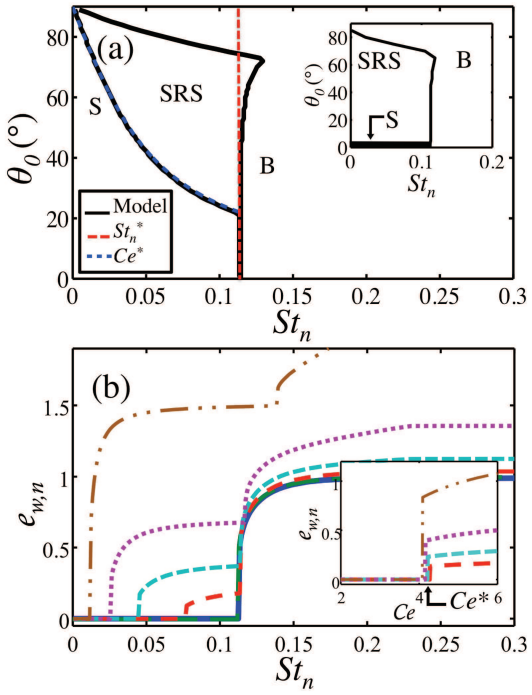

FIG. 4. Theoretical predictions for untethered collisions (no strings): (a) outcome regime map and (b) normal restitution coefficient for collisions with $e_{dry} = 0.99$, $x_0 = 8\ \mu m$, $x_b = 8\ \mu m$, $x_b = 0.2\ \mu m$, $a = 50\ \mu m$, $\mu = 2$ Pa·s, $m = 5.2 \times 10^{-6}$ g, $\sigma = 0.025$ N/m, $p_{gt} = 20$ MPa, $V = 0.1$ and $\theta_0 = 0°$, 15°, 30°, 45°, 60°, and 75° (bottom to top). The dimensionless numbers $Ce^* = 4.2$ and $St_n^* = 0.11$ serve as boundaries for the stick outcome. The inset of (a) shows the predictions without capillary forces, where only normal collisions agglomerate. In (a), the Ce^+ line is nearly identical to the model line, making it difficult to distinguish.

Our identification of importance of capillary forces in oblique collisions leads to a new dimensionless number that, together with St, is key to predicting agglomeration vs. de-agglomeration. Since the transition between stick and stick-rotate-separate occurs when centrifugal forces dominate over capillary forces, a relevant dimensionless number is proposed that we call the centrifugal number,

$$Ce = \frac{m\omega_0^2}{\sigma} \quad , \tag{1}$$

where $\omega_0 = v_{n,0} \tan\theta_0/(4a)$ is the initial angular velocity. (Note that similar to the Weber number (We), Ce is a ratio of inertial to surface-tension forces though, unlike We, Ce refers to inertia stemming from rotation of doublet.) In Fig. 4a, dashed lines corresponding to a critical value of Ce, namely $Ce^* = 4.2$, and a critical value of St_n ($St_n^* = 0.11$), are plotted on top of the theoretical predictions. The two lines enclose the stick region (agglomeration) superbly.

To investigate the collision dynamics in more detail, the predicted wet normal restitution coefficient, $e_{w,n}$ is plotted against St_n in Fig. 4b. In this work, $e_{w,n} = -\vec{v}_f \cdot \vec{n}_f(\vec{v}_0 \cdot \vec{n}_0)$, where the subscripts 0 and f denote pre- and post-collisional values, respectively [18]. Note that this definition distinguishes between the initial and final direction of $\vec{\boldsymbol{n}}$, the unit vector that points between particle centers. The curve for $\theta_0 = 15°$ collisions is almost indistinguishable from normal collisions ($\theta_0 = 0°$), and only stick ($e_{w,n} = 0$) and bounce are observed. At higher angles, the curves also exhibit stick-rotate-separate outcomes (moderate St_n), for which the curves are qualitatively different than in the bounce outcome (higher St_n^*), and a discontinuity in the slope at $St_n^* = 0.11$ separates the two outcomes. The relevance of Ce is further illustrated by the inset of Fig. 4b, which shows $e_{w,n}$ versus Ce for the subset of impact angles large enough so that only centrifugal forces facilitate rebound (no normal reversal criterion is met). The value of Ce^* depends little on impact angle. Moreover, doubling the values of V, x_0, μ, σ, m and a leads to a change in Ce^* by factors of 1.0, 0.79, 0.99, 1.01, 1.01 and 1.13, respectively. Therefore, large changes in inputs result in small changes in Ce^*. This lack of sensitivity of Ce^* has important implications in practical flows. For example, for a nonuniform distribution of liquid, a mid-range value of Ce^* is expected to predict agglomeration well in this regime ($St_n < St_n^*$).

A remarkable aspect of Fig. 4b is that $e_{w,n} > 1$ in some regions, indicating that the normal component of the post-collisional relative velocity is greater than its pre-collisional value. This restitution coefficient typically ranges between zero (perfectly elastic collision) and one (perfectly inelastic). One exception is oblique, dry collisions of a hard particle impacting a soft wall, where $e_{wm} > 1$ has been observed for collisions past a critical impact angle, which is related to the local deformation of the wall [18,19]. However, this same mechanism is not relevant for (dry) particle-particle collisions. For wetted particles with initial separation x_0, the final rupture distance x_f is larger due to stretching of the liquid bridge. The moment of inertia of the doublet, $I = ma^2((\frac{x}{a} + 4)^2 + \frac{32}{5})$, increases as x increases, and, since angular momentum ($I\omega$) is conserved, the angular velocity decreases. Therefore, since the total kinetic energy is $\frac{1}{2}I\omega^2 + \frac{1}{2}mv_n^2$, v_n must increase as the rotational kinetic energy decreases, if we ignore viscous dissipation. So, when the increase in the normal velocity due to this hysteresis in the initial and final separation distance is greater than the amount lost due to viscous dissipation, the magnitude of final normal velocity will be larger than the initial value, leading to $e_{w,n} > 1$. This effect may be relevant in other systems of agglomerates that exhibit hysteresis in the initial and final separation distance, such as nanoclusters where the object shape may deform.

In conclusion, we have used an experimentally validated theory to study agglomeration/de-agglomeration in oblique, wetted collisions. In addition to the stick and bounce outcomes observed for head-on collisions, a new outcome has been observed for oblique collisions in which particles initially agglomerate, and then later de-agglomerate due solely to centrifugal forces. Furthermore, even at high Ca, capillary forces are surprisingly essential for agglomeration in oblique collisions. The relative importance of centrifugal and capillary forces is characterized by a new dimensionless number, the centrifugal number, Ce. For oblique collisions, Ce and the previously established St_n are essential for characterizing agglomeration vs. de-agglomeration, where only St_n is important for normal collisions. In many-particle systems, oblique collisions are the norm, so this introduction of Ce is key to predicting agglomeration vs. de-agglomeration. Similar dimensionless numbers may find use in other agglomerating

systems, by replacing the capillary force in Ce by a measure of the relevant cohesive force (for instance, the van der Waals force). Not only do the dimensionless numbers Ce and St_n aid in our physical understanding, but the associated computational costs of modeling bulk flow by solving the equations for each individual particle via Discrete Element Modeling (DEM) simulations can be simplified with knowledge of the dominant physics. Additionally, we observed a normal restitution coefficient above unity, where the normal relative velocity increases at the expense of angular kinetic energy. This mechanism is not limited to wetted collisions, but is possible in any collision in which the initial separation distance is smaller than the final separation distance, such as in the collision of viscoelastic drops. The micro-level understanding of the physical mechanisms of wetted particle collisions, as investigated here, is essential for a macro-level understanding of diverse systems from pharmaceuticals to interstellar grains.

ACKNOWLEDGMENT

This work was supported by NSF (CBET 0754825 and a REU supplement). We thank Will Brewer for assisting with the experiments.

[1] H.M. Jaeger, S.R. Nagel, and R.P. Behringer, Physics Today **49**, 32 (1966).

[2] G. Barnocky, R.H. Davis, Physics of Fluids **31**, 1324 (1988).

[3] R. H. Davis, D.A. Rager, and B.T. Good, J. Fluid Mech. **468**, 107 (2002).

[4] S. Antonyuk, S. Heinrich, N. Deen, and H. Kuipers, Particuology **7**, 245 (2009).

[5] C.M. Donahue, C.M. Hrenya, R.H. Davis, K.J. Nakagawa, and A.P. Zelinskaya, J. Fluid Mech. **650**, 479 (2010).

[6] A.A. Kantak and R.H. Davis, J. Fluid Mech. **509**, 63 (2004).

[7] B.J. Ennis, J.L. Li, G.I. Tardos, and R. Pfeffer, Chem. Eng. Sci. **45**, 3071 (1990).

[8] C.M. Sorace, M.Y. Louge, M.D. Crozier, V.H.C. Law, Mech. Research Com. **36**, 364 (2009).

[9] F.L. Yang and M.L. Hunt, Phys. Fluids **18**, 121506 (2006).

[10] C.M. Donahue, C.M. Hrenya, and R.H. Davis, Physical Review Letters **105**, art. no. 034501 (2010).

[11] A.A. Kantak and R.H. Davis, Powder Tech. **168**, 42 (2006).

[12] C.M. Donahue, W.M. Brewer, R.H. Davis, C.M. Hrenya, J. Fluid Mech. (in press).

[13] T. Mikami, H. Kamiya, and M. Horio. Chem. Eng. Sci. **53**, 1927 (1998).

[14] M.E. O'Neill and R. Majumdar, ZAMP **21** 164 (1970).

[15] P. Darabi, K. Pougatch, M. Salcudean, and D. Grecov, Chem. Eng. Sci. **64**, 1868 (2009).

[16] R. Petela, Fuel **70**, 509 (1991).

[17] G.P. Lian, C. Thornton, and M.J. Adams, J. Colloid and Interface Sci. **161**, 138 (1993).

[18] K. Saitoh, A. Bodrova, H. Hayakawa, and N. V. Brilliantov, PRL, **105**, 238001 (2010).

[19] M.Y. Louge and M.E. Adams, PRE **65**, 021303 (2002).